Performance Assessment and Failure Prediction of Corroded Cast Iron Pipes

P. Rajeev[1] and D. J. Robert[2]
[1]*Department of Civil & Construction Engineering, Swinburne University of Technology, Melbourne, Australia*
[2]*School of Civil, Environment and Chemical Engineering, RMIT University, Melbourne, Australia*
E-mail: prajeev@swin.edu.au

ABSTRACT: The increasing failure rate in deteriorating pipe and unplanned failures will increase economical loss and social impact. One of the important tasks in the asset management framework is to estimate the pipe stress of a certain pipe section subjected to operational loads and corrosion. These factors may, however, be considered uncertain not only at a given point of time, but also have substantial time variance. The probability of structural failure of pipes can be estimated using Monte Carlo type simulation conjunction with pipe stress analysis models. This paper assess the pipe performance using different pipe stress prediction models and 3-D finite element analysis. Further, the effect of corrosion was modelled and incorporated with stress prediction models to assess the pipe performance over the lifetime. Finally, the probability of failure was computed and discussed in application with a case study of buried cast iron pipe subjected to external corrosion and loadings.

KEYWORDS: Cast iron, corrosion, pipe, probability of failure, asset management, numerical analysis

1. INTRODUCTION

Pipelines are the one of the important infrastructure transporting the water and gas from one location to other. The failure of aging infrastructure is the major problem for Australia and around the world. The failure of buried pipeline depends on several factors such as soil corrosion, traffic load, and pressure loads (Rajeev et al. 2014). In a buried pipe, the structural load carrying capacity of pipe deteriorates mainly due to both external and internal corrosions (i.e., corrosion causes the reduction in pipe wall thickness that increases the pipe stress).

The external and internal loadings (i.e., traffic load and internal water/gas pressure) cause the pipe stress, which may increase with time due to increase in demand and time dependent corrosion. The pipe fails when the stress on pipe exceeds the pipe stress capacity. The failure mode depends on several factors such as type of loading, level of loading, level of deterioration, type of pipe material and pipe geometry and can be explained using “Schlik diagram”. The large dimeter (i.e., diameter > 300 mm) pipe failure data of five major water utilities in Australia were analysed in Rajeev et al. (2014) and revealed that the corrosion is the main cause for most of the pipe failures. Similarly, the failure analysis of high-pressure natural gas was conducted by Hassan et al. (2007) and Hemandez- Rodridriguez et al. (2007) who concluded that the corrosion as the major factor to cause failure of buried gas pipe. Various corrosion models were developed to model the long-term corrosion in buried pipe. Most of those models are empirical or semi-empirical and the model parameters are calibrated to fit the data collected from either laboratory tests or field or both. However, the variation in model prediction and the actual corrosion, which depends on soil type and climatic condition, is large (e.g., Petersen and Melchers, 2016). The corrosion effect needs to be modelled accurately to predict possible future failures.

In addition, the knowledge of the stresses to which pipes are subjected is essential to understand the in-service pipe failures. Further, the condition of the backfill soil significantly affects the generated stress in the pipe as it acts as the medium of protection from external traffic load and internal water pressure. There are various analytical and semi-empirical pipe stress prediction models, available at present, such as those developed by Sprangler (1941) and Watkins (1998). Though these models are widely used in practice, the models involve various assumptions and limitations, for instance, the negligence of three dimensional effects and the use of Winkler springs to analyse pipe-soil interaction. A more advanced approach is to solve the problem using 3-D finite element analyses to determine the stress distribution for a pipe at hand with a specific set of external internal factors (Robert et al, 2016). However, this process can be very time consuming and also would require specialised skills and resources in computer analysis of soil/structure interaction. Hence, in present day’s design, the estimation of pipe stress due to internal and external loadings is mainly performed on the basis of available analytical/empirical models. In the current study, the pipe responses from the analytical/empirical models are compared with 3-D finite element (FE) analysis conducted for different pipe geometry, operating conditions and embedded states (i.e. soil condition). Results of the analysis are used to identify the situations where the analytical model predictions of the pipe response are applicable, over-conservative and involve high risk of failures. Further, the effect of corrosion models in pipe failure prediction is also explored and the sensitivity of the model parameters are examined. The probability of structural failure throughout the life of the pipe is estimated using Monte Carlo simulation, the first-order reliability method (FORM) for buried cast iron pipe subjected to external corrosion and loading as a case study. Finally, the effect of corrosion and the stress analysis models on the failure perdition of buried pipe is discussed.

2. CORROSION MODELS

Over the years, several corrosion prediction models were developed for buried water and gas pipes and used by the utilities for their network renewal plan. The corrosion model for buried pipe correlates the growth of corrosion pit geometry (mostly corrosion pit depth) with time to the surrounding soil properties. The growth of corrosion pit significantly depends on soil condition, pipe material and climatic condition of the location; therefore, a unique model cannot be used to predict the effect of corrosion in buried pipe. For example, Dolaec et al. (1980) proposed a power function to correlate “pit depth” with the age of pipe; while, Randall-Smith et al. (1992) concluded that corrosion pit grow at a constant rate and expressed a linear model. Kurcea and Mattson (1987) derived corrosion model to predict the pit depth of buried cast iron pipe as in Eq. (1).

$$d = K\tau^{n} \quad (1)$$

where, K and n are constants and normally assumed to be equal to 2 and 0.3 respectively.

Rajani et al. (2000) developed a two-phase corrosion model as given by Eq. (2) to predict the pit depth over exposure time period of buried cast iron pipe in varying soil corrosivity.

$$d = a\tau + b(1 - e^{-c\tau}) \quad (2)$$

where, d is the corrosion pit depth, a is the minimum corrosion rate (mm/yr), k is the pitting depth constant (mm) and c is the corrosion rate inhibition factor (yr^{-1}), and τ is exposure time period. The possible range of a is 0.0042 to 0.0336, b is 1.95 to 15.6 and c is 0.01 to 0.18 for all type soils. As explained in Rajeev et al. (2015), Figure 1 shows the all possible corrosion pit depth with exposure time for combination of maximum and minimum corrosion model parameters. The predicted corrosion pit depths show significant variation and the variability increases with exposer time. Hence, the failure prediction also shows large variability, which may mislead asset management decision-making process. In order to handle the variability, appropriate probabilistic methods should be integrated with the physical model to propagate associated variable uncertainty and estimate reliable asset management decision.

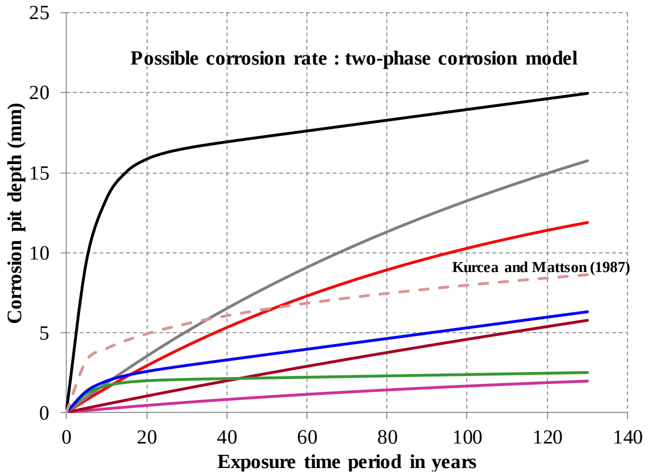

Figure 1 Variability in the corrosion pit depth with exposure time

3. PIPE STRESS PREDICTION MODELS

The structural failure of pipe occurs when the stress demand on pipe is exceed the stress capacity of the pipe material. Therefore, it is essential to estimate the level of stress in pipe and its variation with time for the safe operation. A range of pipe stress prediction models were developed and are used in design of new pipeline and failure assessment of in-service pipelines. As stated above, the performance and failure of buried pipe is controlled by various factors such as: (1) internal pressure leads to busting of pipe; (2) external load (i.e., traffic and soil) leads to crushing and local buckling of pipe; and (3) corrosion leads to reduction in wall thickness and leakage. The existing pipe stress prediction equations take into account one or more of these factors and make simplified assumptions in the prediction. Therefore, significant level of variations exists among the predicted stress, which may lead to undesirable failures. Details of different stress prediction model can be found elsewhere (e.g., Robert et al., 2015). However, a brief summary of stress prediction model is provided below for brevity.

Based on 2D ring theory, a simple stress prediction model was developed by neglecting the ring deflection (i.e., rigid pipe). The stress due to traffic and soil loads are assumed to be a uniform stress at the pipe crown level. The model is capable of accounting the lateral soil support based on the trench type, backfill material and level of compaction by selecting a suitable earth pressure coefficient. The Eq. (3) predicts the maximum bending stress in the pipe ($\sigma_{b,max}$).

$$\sigma_{b,\max} = \frac{k \cdot q \cdot D}{2 \cdot t} + 1.5 \cdot (1-k)\frac{q \cdot D^2}{4 \cdot t^2} \qquad (3)$$

where, σ_{max} is the maximum bending stress in the pipe, q is the uniform vertical stress due to soil and traffic loads, D is the pipe diameter, t is the pipe wall thickness and k is the lateral earth pressure coefficient. The Boussinesq solution can be used to estimate the q due to traffic load.

However, the deflection of the ring is often the most important consideration in flexible pipe design and it requires accurate determination of stresses around the pipe due to soil and traffic loads. The Spangler stress formula and the modified Iowa formula are typically used in the design of buried flexible pipes. The Spangler stress formula computes the circumferential bending stress at the pipe invert due to vertical load as follows (e.g., Masada, 2000):

$$\sigma_{b,\max} = \frac{3 \cdot K_b \cdot W_{vertical} \cdot E \cdot t \cdot D}{E \cdot t^3 + 8 \cdot K_z \cdot P \cdot D^3} \qquad (4)$$

where $W_{vertical}$ is the vertical load due to backfill and surface loads including an impact factor, E is the pipe modulus of elasticity and P is the internal pressure. K_b and K_z are bending moment and deflection parameters, respectively, that depend on the bedding angle. The appropriate values of K_b and K_z can be found in Moser and Folkman (2008).

In 1941, Spangler combined the elastic ring theory and his unique "fill-load hypothesis" to establish the original Iowa formula to estimate the pipe ovality due to vertical loads. The fill-load hypothesis consisted of three elements: (1) The vertical load on a pipe may be determined by Marston's theory and is distributed approximately uniformly over the crown pipe width; (2) The vertical reaction on the bottom of a pipe is equal to the vertical load on the pipe and is distributed approximately uniformly over the invert pipe width; (3) The passive horizontal pressure on the side of the pipe is distributed in a parabolic shape over the middle 100^0 of the pipe and the maximum unit pressure is equal to the modulus of passive pressure of the side fill material multiplied by one-half of the horizontal deflection of the pipe.

Based on the assumed stress distribution, the Iowa formula was derived as follows:

$$\Delta x = \frac{D_L W_{vertical} r^3 K_z}{EI + 0.061E' r^3} \qquad (5)$$

where, Δx is the horizontal diameter change, D_L is the time lag factor, I is the moment of inertia of pipe, r is pipe radius and E' is the modulus of passive soil resistance. The time lag factor D_L was introduced to recognize a slight increase in pipe deflections over time due to consolidation of the soil existing at the sides of the pipe. The values for D_L, K_b and K_z can be found elsewhere (Masada, 2000).
The original Spangler formula given in Eq. (4) does not include the beneficial effects of lateral soil restraint. By combing the original Spangler formula and the Iowa formula, Warman et al. (2006) proposed a modified Spangler equation as follows:

$$\sigma_{b,\max} = \frac{6 \cdot K_b \cdot W_{vertical} \cdot E \cdot t \cdot r}{E \cdot t^3 + 24 \cdot K_z \cdot P \cdot r^3 + 0.732 \cdot E' \cdot r^3} \qquad (6)$$

The stress is the pipe due to internal pressure (σ_p) can be computed using Eq.(7).

$$\sigma_p = \frac{PD}{2t} \qquad (7)$$

Therefore, the total stress in the pipe is the combination of bending and pressure (i.e., $\sigma_T = \sigma_p + \sigma_{b,max}$).

4. PIPE STRESS ANALYSIS USING FINITE ELEMENT METHOD

Three dimensional (3D) finite element analyses were carried out using ABAQUS 6.11/ standard to obtain the pipe and soil stress distribution around the pipe, and to assess the predictions from analytical models. The soil was represented by 8-noded brick reduced integration elements and the pipe was represented by 8-noded shell reduced integration elements. The behaviour of both soil and pipe were assumed as a linear elastic material similar to what is assumed in the derivation of available analytical solutions. i.e., soil is assumed to be over-consolidated and behave elastically during the range of tested traffic loads. The soil side boundaries of the FE model were assumed to be smooth and are located far (i.e., 5m) from the pipe (& traffic loads) to eliminate any boundary effects. Figure 2 shows the mesh discretization (6,600 shell elements and 108, 000 solid elements to represent the pipe and soil, respectively) and model dimensions. The appropriate dimensions and the mesh density of the model were selected after a number of trials to minimise mesh and boundary effects on the calculated pipeline stresses. In line with the analytical solutions, the interaction between pipe and soil was assumed to be frictionless, and the traffic loads were simplified to point loads. The results obtained from the numerical models are compared with the predictions from the analytical models in terms of soil and pipe stresses.

4.1 Analysis plan

Three series of 3D FE analysis were conducted to investigate the reliability of the predictions from analytical models during the application of external loads (i.e traffic loads). Firstly, the analysis were conducted on the basis of a cast iron pipe (Diameter=660mm, thickness=8mm, Stiffness=100GPa) buried at a depth of 0.8m in soft soil (Stiffness = 2MPa) to investigate how well the analytical models can capture different lateral support effect from soil (i.e. effect of lateral soil earth pressure coefficient). In the second series, analyses were performed to compare the stress distributions of pipes having various diameter to thickness ratio (D/t) buried in different soil conditions (i.e. compaction levels). Here, the cast iron pipes of diameters 300mm and 660mm with thicknesses of 8mm, 10mm, 15mm and 27mm were considered in conjunction with soft soil (Stiffness=10MPa) and hard soil (Stiffness=50MPa). Analyses were also performed to examine the effects of different axle load configurations on pipe stress distribution in comparable with analytical model predictions. A pavement system consisting of top down, asphalt (thickness = 240 mm, modulus = 3 GPa), unbound base (thickness =100mm, and modulus = 300 MPa), and subgrade (deep, modulus=50 MPa) was considered in this case. A cast iron pipe having similar geometry and properties with series 1 was considered in the third series. An axle load of 80kN (single axle dual tyre) was considered. Summary of the analysis plan is presented in Table 1.

Table 1 FE analysis details

Analysis Series	Objective	Parameters (Range)
1	Investigate Lateral soil support effect	k=0.1-1.0
2	Investigate D/t effect on various compacted soils	D/t=10-40 Soil modulus=10MPa, 50MPa
3	Comparison of FE predictions with Analytical model predictions	Analytical models: Sprangler, Ring, Modified Ring model

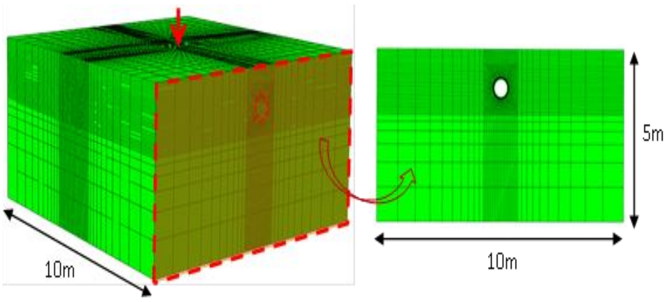

Figure 2 Model dimensions and mesh discretization of the finite element model

4.2 Finite Element Analysis Results

4.2.1 Effect of lateral soil resistance

A series of 3-D FE analyses was performed to investigate the effect of lateral soil support (lateral soil earth pressure coefficient, k =0.1, 0.25, 0.42, 0.65 & 0.97) on maximum pipe stress due to the application of traffic loading. The maximum pipe stress computed from the FEM simulation is compared with the predictions from the analytical models by Sprangler (Eq.6) and the elastic ring model (Eq. 3) and shown in Figure 3. The ring model, which caters for the variation of lateral earth pressure, predicts the trend of the pipe stress variation similar to the FEM prediction and the predicted stresses show close match, when the k value varies within 0.4 to 0.6. However, the ring model over and under predicts the stress for k values less than 0.4 and higher than 0.6, respectively. Sprangler model predicts similar pipe stress with FE model for subgrade soils with internal friction angle of 35^0 (i.e., k=0.42). Figure 4 (a and b) shows the comparison of vertical and horizontal stress distribution in soil directly above the pipe in lateral direction and adjacent to the pipe in vertical direction respectively. The 3D vertical stress analysis shows peaking of stress under the traffic load and decay of stress in both vertical and horizontal stresses at the pipe level. In contrast, the vertical soil stresses predicted by the Spangler model is nearly 30% higher than the FEM results, while the ring model stress is close to average stress of the FEM prediction. As shown in Figure 4 (a), the horizontal stress prediction from FE analysis is substantially different from the assumption used in ring model (i.e., horizontal stress = *k* x vertical stress) and Sprangler model.

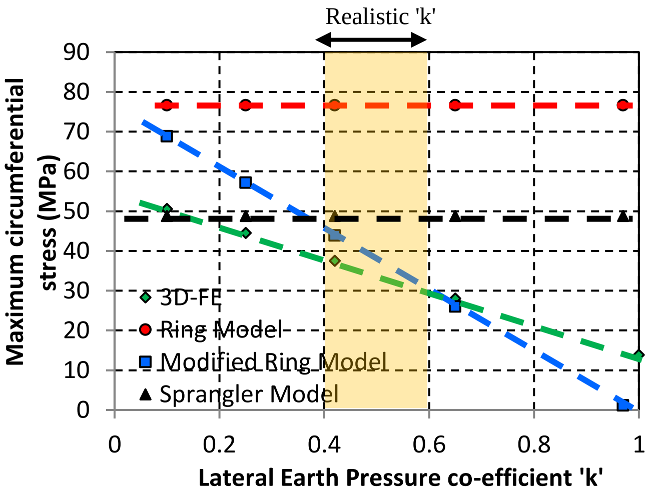

Figure 3 Maximum circumferential stress of the pipe under different lateral resistance of soils

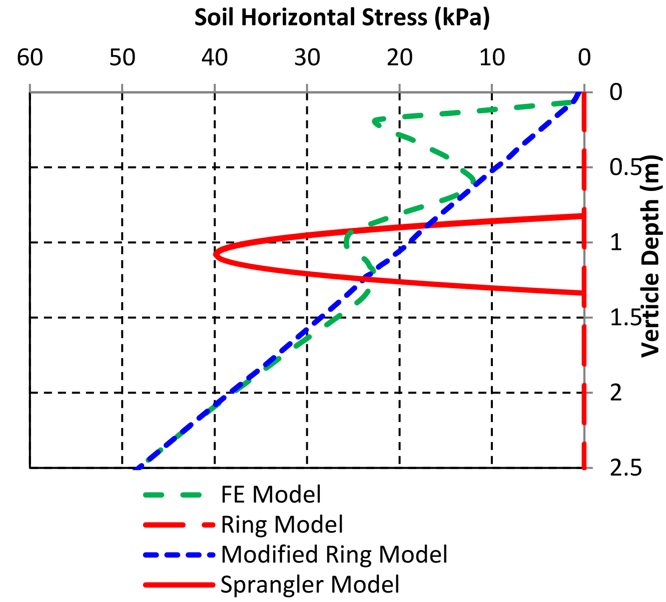

(a) Horizontal soil stress

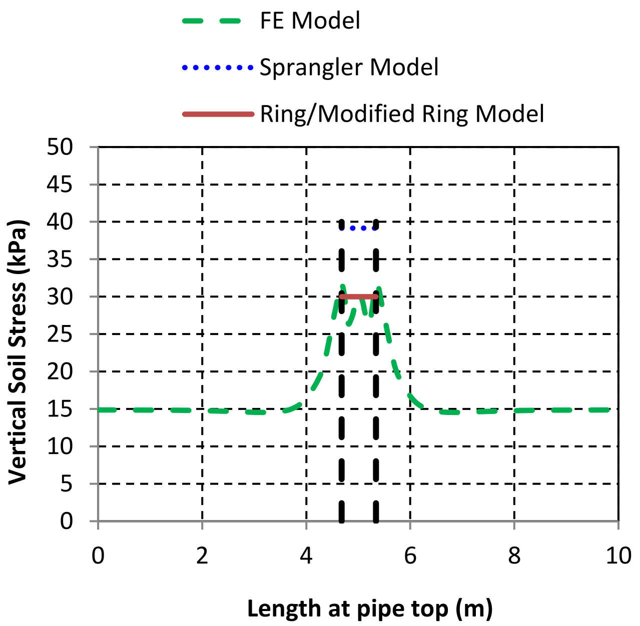

(b) Vertical soil stress

Figure 4 Horizontal and vertical soil stresses adjacent to the pipe

4.2.2 Effect of pipe geometry

The results of the analyses conducted to investigate the effects of pipes having various pipe diameters (i.e., 300 mm and 660 mm) to thickness ratio (D/t) buried in different soil conditions (i.e., compaction levels) are showed in Figure 5. In general, the maximum pipe stress stresses due to traffic loading increases with the D/t ratio. Sprangler model predicts similar maximum pipe stresses compared to 3D FE analysis for larger diameter pipes buried in soft and hard soil conditions (Figures 5a & b). On the other hand, the predictions from Ring and modified Ring model significantly over-predicts the maximum pipe stresses for the large diameter pipes due to their limitation in capturing the realistic soil and pipe deformations for large diameter pipes. However, Ring model and modified Ring model predict similar pipe maximum stresses compared to 3D FE results for smaller diameter pipes buried in soft and hard soils respectively. These findings reveal that the Ring model predictions could be applicable for small diameter pipes buried in soft soils (i.e. less lateral support), while the predictions from modified Ring model could be used for small diameter pipes buried in hard soil.

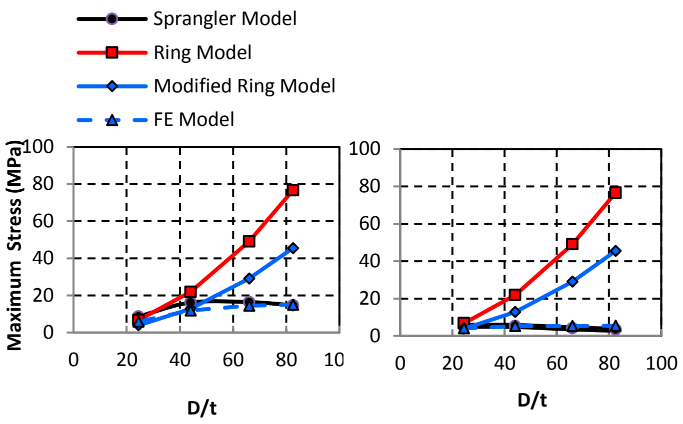

(a) D660 – E10 MPa (b) D660 – E50 MPa

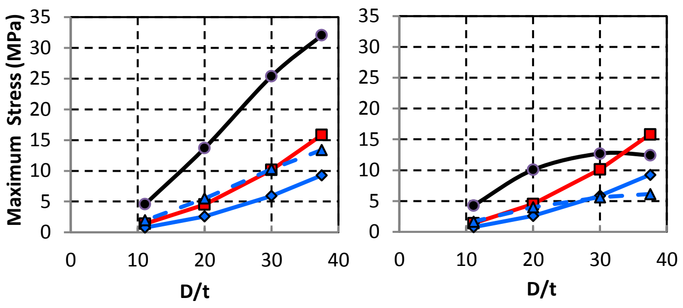

(c) D300 – E10 MPa (d) D300 – E50 MPa

Figure 5 The effect of traffic loading on pipes buried in different soil conditions

4.2.3 Development of stress prediction model

A series of 576 finite element simulation was performed considering varying level of traffic load, internal pressure, soil modulus, soil density, lateral earth pressure coefficient, pipe diameter, pipe wall thickness, and burial depth. The maximum stress in the pipe was determined from the finite element analysis for all the possible combinations of the variable. The details of the finite element simulation can be found in Robert et al. (2016).

The response surface method is used to develop the functional relationship between the maximum pipe stress and the variable. The detail procedure of model development and parameter calibration can be found in Merrin et al. (2014). The following pipe stress prediction equation was developed:

$$\sigma_{T,\max} = \beta_0 + \beta_1\left(\frac{PD}{t}\right) + \beta_2\left(\frac{W}{h\cdot t\cdot E_s}\right) + \beta_3\left(\frac{W}{h\cdot t\cdot k}\right) + \beta_4\left(\frac{W}{h\cdot t\cdot p}\right) \quad \text{(in MPa)} \qquad (8)$$

where, β_0 = 7.7256, β_1 = 0.422, β_2 = 22.455, β_3 = 0.0233 and β_4 = -0.2512.

5. PERFORMANCE ASSESSMENT OF PIPE

The long-term performance assessment of pipelines depends on the integrating the engineering demand, structural capacity of the pipe and its variations with time. In metallic pipes, the structural capacity of a pipe deteriorates with time due to both external and internal corrosions. While the stress demand on the pipe may varies over time due change in pumping pressure and traffic conditions. As explained above, the structural failure occurs when the capacity reduces below the demand on the pipe.

Due to larger variability in demand prediction models (i.e., stress prediction) and corrosion models, probabilistic approaches can be integrated with the physical models to reliably estimate the performance. Therefore, the annual probability of failure of pipeline can be estimated as:

$$\lambda = P(D \geq C) \tag{9}$$

where, λ is annual probability of failure, $P(.)$ probability of failure, D is the demand and C is the capacity.

In this study, the stress prediction model is integrated with the corrosion models to estimate the probability of failure with time. The variability in corrosion model parameters and the prediction of pipe stress methods are treated as random variables. Monte Carlo simulation with optimised Latin hypercube sampling (OLHS) technique is used to generate random combination of corrosion models with stress prediction models. The uncertainty in the demand and capacity models can be effectively quantified using OLHS, which provides a stratified sampling scheme rather than the purely random sampling, as it provides more efficient means of covering the probability space (Rajeev and Tesfamariam, 2012). Detail of OLHS and its application can be found elsewhere (e.g., Park, 1994; Rajeev et al, 2013). The first-order reliability method (FORM) is used to compute the probability of failure, which is then used to analyse the performance.

5.1 Computation of probability of failure

Reliability is defined as the probability of success of a system under a given loading condition. In design, the reliability of a system component is evaluated with respect to one or more limit states. For example, in this problem, the limit state can be defined in terms of vertical deformation along the pipeline. Let's assume that the system is described by a set of basic variables x, (e.g., pipe material properties, soil stiffness and operational condition). The possible realisation of x can be separated into two sets on the basis of the considered limit state, namely the safe set for which the system is safe and the failure set for which the system fails or defined to be in a failure state. The surface separating the safe set and the failure set in the space of basic variables is denoted the limit state surface G(x), and the probability of failure can be defined with respect to the limit state surface as given in Eq. (10).

$$P_f = P\left(G(\mathbf{x}) \leq 0\right) = \int_{G(\mathbf{x}) \leq 0} f_x(x)\, dx \tag{10}$$

where $f_x(x)$ is the joint probability density function for x. This expression is often referred to as the probability integral over the failure set. The complement, $1\text{-}P_f$, is accordingly referred to as the reliability. The corresponding reliability index β is determined by

$$\beta = -\Phi^{-1}(P_f) \tag{11}$$

where Φ is the standard normal distribution function.

The probability of failure and the reliability index can be estimated by a reliability method which can be any amongst several available analytical methods such as first- and second-order reliability methods (i.e., FORM & SORM) as well as the simulation methods (Harr, 1987; Baecher and Christian, 2003).

In this study, both the analytical methods (i.e., FORM) and simulation method (i.e., Monte Carlo simulation using Latin Hypercube Sampling technique) were used to study the reliability of offshore pipeline. The FORM, Monte Carlo simulation and Latin Hypercube Sampling technique are briefly explained in the sections below.

In First Order Reliability Methods (FORM), the limit state function G(x) is linearized to compute the first two moments (i.e., mean and variance) as a function of x. However, in the vast majority of real situations, the limit state function is not linear. In this case, the first two moments of $G(x)$ cannot be determined on the basis of the corresponding moment of x only, and their joint distribution is needed. The computation of reliability index for nonlinear $G(x)$ can be found elsewhere (e.g., Pinto et al., 2004).

FORM requires a simplified relationship for $G(x)$ is required which is some time either difficult to establish or the established relationships are too complicated to perform the analytical reliability methods. The relationship can be established using the concept of response surface method (RMS). Then, the response surface model, with combination of FORM approach, can be used for the calculation of reliability index values using the following expression [Baecher and Christian (2003)]

For uncorrelated normally distributed R and S

$$\beta = \frac{\mu_R - \mu_S}{\sqrt{\sigma_R^2 + \sigma_S^2}} \tag{12}$$

For uncorrelated lognormally distributed R and S

$$\beta = \frac{\ln\left[\dfrac{\mu_R}{\mu_S}\sqrt{\dfrac{1+CoV_S^2}{1+CoV_R^2}}\right]}{\sqrt{\ln\left[\left(1+CoV_S^2\right)\left(1+CoV_R^2\right)\right]}} \tag{13}$$

where R is the resistance (or capacity) of a system, S is the load (or demand) on the system and CoV is the coefficient of variance.

6. CASE STUDY

In order to quantify the effect of uncertainty in the prediction of demand and capacity of buried pipe on the safety, the time dependent reliability index and the probability of failure was computed for a pipe section with the diameter of 600 mm and wall thickness of 25 mm, as explained in section 5. The complex corrosion process in buried pipe and loading often involve input data or parameters from field and laboratory testing and sometime expert opinion based on experience and judgment.

Table 2 shows the possible ranges and the most likely values of the input variables such as pipe material properties, soil properties, traffic and pressure loads and corrosion model parameters. In order to perform the traditional probabilistic analysis, an appropriate probability distribution function has to be identified for each input parameter on the basis of the available data. In this study, the input parameters are assumed to follow the uniform distribution due to lack of information of input parameters. A set of random sample was drawn from assigned distribution and the sample size is around 5000. The pipe stress is calculated for each set of random variable at present and with exposure time by incorporating the random corrosion model that also sampled. No variability is assumed for the pipe diameter and the ultimate tensile capacity of the pipe material. Pipe material is cast iron.

Table 2 Input parameters for pipe, soil, load and corrosion model

Parameter	Minimum	Most likely	Maximum
Pipe diameter, *D* (mm)	-	600	-
Wall thickness, *t* (mm)	20	25	30
Burial depth, *h* (mm)	300	800	1500
Ultimate tensile capacity, σ_{ult} (MPa)	-	100	-
Elastic modulus of pipe, *E*, (GPa)	-	180	-
Lateral earth pressure coefficient, *k*	0.2	0.4	0.6
Soil elastic modulus, *E'*, (MPa)	2	25	50
Soil unit weight, γ (kN/m^3)	18	20	24
Traffic, *W* (kN)	20	40	70
Pressure, *P* (kPa)	300	600	1000
Corrosion model Eq. (2)			
a	0.0042	0.009	0.0336
b	1.95	6.27	15.6
c	0.01	0.14	0.18
Corrosion model Eq.(1)			
K	1.7	2.0	2.3
n	0.255	0.3	0.345

The pipe stress was obtained using the modified Spangle model, 2D ring model and analytical model derived using 3-D FE data. The time dependent stress was calculated incorporating the corrosion models in Eqs. (1) and (2). The reliability index was calculated using the 5000 pipe stress values for each models and each year. The FORM (Eq. 12), in which the mean and the standard deviation in demand were estimated using 5000 stress values, was used to compute the reliability index. The Eq. (11) was used to compute the probability of failure. The computed reliability index and probability of failures and the time dependent variation on this parameters are shown in Figures 6 and 7.

As seen from Figures 6 and 7, the estimated time dependent reliability index/ probability of failure have significant dependency on the stress analysis method and corrosion model. For example, the reliability index is as high as 10 at the year 1 and decreases rapidly with time and drops below 0.1 after 100 years, when the 2D ring model combined with the corrosion model given in Eq.(2).

However, the effect of corrosion model is less when the Spangler methods is used for stress analysis combined with any of the corrosion model.

The reliability index at the design level is significantly high for 2D ring model, however, the index is dropping rapidly depending on the corrosion model. The reliability index computed using the stress prediction model using FE analysis (Eq. 8) is higher than both the ring model and Spangler model. Therefore the probability of failure is very low during the design life (i.e., <100 years), however, the probability failure increases rapidly after 100 years as seen in Figure 7 (blue line).

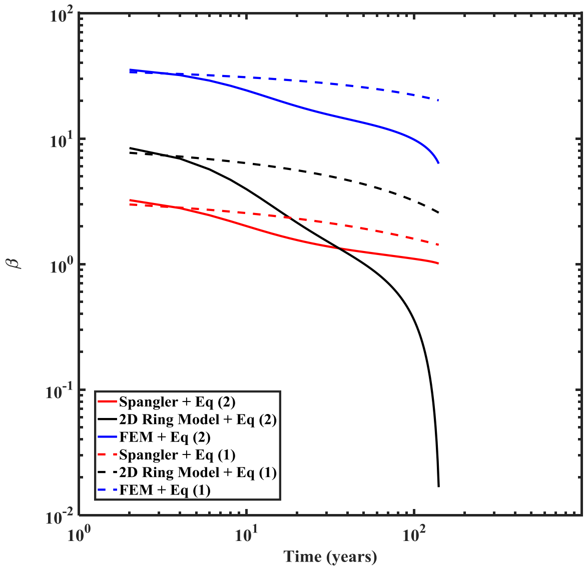

Figure 6 Computed reliability index and variation with time and section of stress model

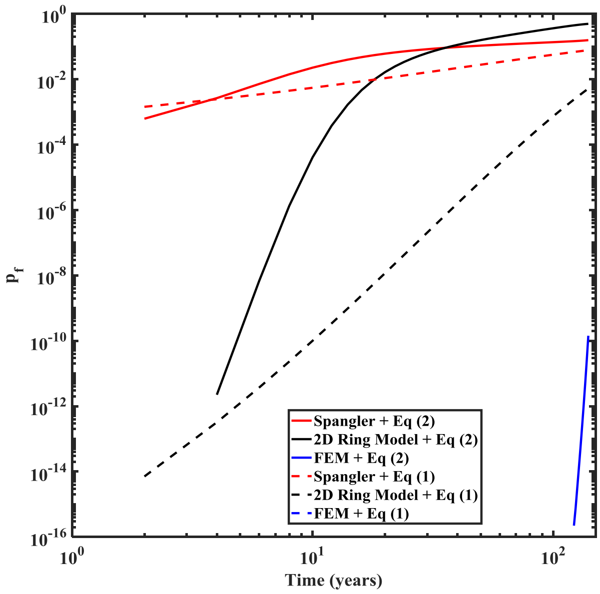

Figure 7 Computed probability of failure and variation with time and section of stress model

7. SUMMARY AND CONCLUSION

In this paper, the long-term performance assessment of buried cast iron pipe is outlined. The effect of stress analysis methods and the corrosion models on the failure prediction was studied. A series of 3D finite element analysis was performed to study the effect of external and internal loadings and the sensitivity of each on pipe geometry and soil properties were explored. Results revealed that pipe stress prediction from analytical model are in-line with FE results only under certain scenarios, but mostly substantial differences were encountered between them. For example, Sprangler model predicts similar maximum pipe stresses compared to 3D FE analysis for larger diameter pipes buried in soft (i.e. k~0.4) and hard soil conditions.

The stress predictions for smaller diameter pipes using the Sprangler model resulted over-estimation of stresses compared to FE model predictions. On the other hand, ring model and modified Ring model predict similar pipe maximum stresses compared to 3D FE results for smaller diameter pipes buried in soft and hard soils respectively. For large diameter pipes, both Ring and modified Ring models over-estimate the pipe stresses compared to numerical model outcomes. Hence the use of analytical solutions to predict maximum pipe stresses can only be conditionally applicable and hence should be used with care. It was also found that the safety assessment significantly depends on pipe stress prediction method and selection of corrosion model. This will affect the design level safety as well as the long-term safety of the buried pipe. Further, the influence of other factors such as soil/pipe non-linearity, pipe lining, and dynamic loadings, which are not considered in this study, can have significant influence on the pipe stress prediction and performance assessment of buried pipes.

8. REFERENCES

Baecher, G. B., and Christian, J. T., (2003) “Reliability and statistics in geotechnical engineering”, Wiley, New York.

Doleac, M. L., Lackey, S. L., and Bratton, G. N., (1980) “Prediction of time-to failure for buried cast iron pipe”, Proceedings of American water works association annual conference, Denver, Co, pp21-28.

Doyle, G., Seica, M. V., and Grabinsky, M. W. F., (2003) “The role of soil in the external corrosion of cast iron water mains in Toronto”, Canada, Can. Geotech. J., 40, pp 225-236.

Hammonds, J. S., Hoffman, F. O., and Bartell, S. M., (1994) “An introductory guide to uncertainty analysis in environmental health and risk assessment. Oak Ridge, TN: SENES Oak Ridge, Inc.

Harr, M. E., (1987) “Reliability-based design in civil engineering”, McGraw-Hill, New York.

Hassan, F., Iqbal, J., and Ahmed, F., (2007) “Stress corrosion failure of high-pressure gas pipeline”, Eng Fail Anal,14, pp 801-809.

Hemandez-Rodridriguez, M. A. L., Martinez-Delgado, D., Gonzalez, R., Perez Enzeta, A., Mercado Solis, R. D., and Rodriguez, J., (2007) “Corrosive wear failure analysis in a natural gas pipeline, Wear”, 263, pp 567-571.

Kucera, V., and Mattson, E., Atmospheric corrosion, In: Mansfeld F, editor. Corrosion mechanics, New York, NY: Mercel Dekker, 1987.

Merrin, J., Hung, H. P., Rajeev, P., Robert, D. J., and Kodikara, J., (2014) “Stress analysis of buried pipes”, 8th Australasian Congress on Applied Mechanics, ACAM 8, Melbourne, Australia.

Moser, A. P., and Folkman, S., (2008), “Buried Pipe Design”, Mc Graw Hill, New York.

Park, J. S., (1994) “Optimal Latin-hypercube designs for computer experiments”, Journal of Statistical Planning and Inference, 39,pp 95-111.

Petersen, R. B., and Melchers, R. E., (2012) “Long-term corrosion of cast iron cement lined pipes”, International Conference in Corrosion and Prevention, Melbourne, Australia.

Petersen, R. B., and Melchers, R. E., (2016) “Predicting the corrosion of cast iron pipes”, Ozwater 2016, Australia.

Pinto, P. E., Giannin, R, and Franchin, P., (2004) “Seismic reliability analysis of structures”, IUSS Press, Pavia, Italy.

Rajani, B., Makar, J., McDonald, S., Zhan, C., Kuraoka, S., Jen, C. K., and Veins, M., (2000) “Investigation of grey cast iron water mains to develop a methodology for estimating service life”, Denver, CO: American Water Works Association Research Foundation.

Rajeev, P., Imteaz, M., and Gad, E., (2015) “Effect of soil corrosion in failures of buried pipes”, Proceedings of Sustainable Solutions in Structural Engineering and Construction, Australia, pp 1-7.

Rajeev, P., Kodikara, J, Robert, D., Zeman, P., and Rajani, B., (2014) “Factors Contributing to Large Diameter Water Pipe Failure as Evident from Failure Inspection”, Journal of Water Asset Management International, 10, Issues 3, pp 9-14.

Rajeev, P., Robert, D. J., Thusyanthan, N. I., and Kodikara, J., (2013) “Reliability Analysis of upheaval bucking of offshore pipelines”, Australian Geomechanics, 48, Issues 4, pp 137-148.

Rajeev, P., and Tesfamariam, S., (12012) “Seismic fragility of non-ductile reinforced concrete frames with consideration of soil structure interaction”, Soil dynamics and earthquake engineering, 40, pp 78-86.

Randall-Smith, M., Russell, A., and Oliphant, R., (1992) “Guidance manual for the structural condition assessment of the trunk mains”, Swindon, UK: Water Research Centre.

Robert, D. Rajeev, P. Kodikara, J. and Rajani, B. 2016, 'An equation to predict maximum pipe stress incorporating internal and external loadings on buried pipes', in Canadian Geotechnical Journal, N R C Research Press, Canada, vol. 53, no. 8, pp. 1315-1331 ISSN: 0008-3674

Spangler, M. G., (1941) “The Structural Design of Flexible Pipe Culverts”, Bulletin 153, Iowa Engineering Experiment Station, Ames, Iowa.